NASA Technical Memorandum 109016

AERODYNAMICS OF A SPHERE AND AN OBLATE SPHEROID FOR MACH NUMBERS FROM 0.6 TO 10.5 INCLUDING SOME EFFECTS OF TEST CONDITIONS

M. LEROY SPEARMAN
AND
DOROTHY O. BRASWELL

AUGUST 1993

National Aeronautics and
Space Administration

Langley Research Center
Hampton, Virginia 23681-0001

AERODYNAMICS OF A SPHERE AND AN OBLATE SPHEROID FOR MACH NUMBERS FROM 0.6 TO 10.5 INCLUDING SOME EFFECTS OF TEST CONDITIONS

M. Leroy Spearman
Langley Research Center
Hampton, Virginia

Dorothy O. Braswell
Langley Research Center
Hampton, Virginia

Summary

Wind tunnel tests were made for spheres of various sizes and for an oblate spheroid over a range of Mach numbers and Reynolds numbers. Tests for the oblate spheroid indicated drag values about 10 percent higher than that for a sphere. The oblate spheroid results also indicated a region at high Mach numbers where inherent positive static stability might occur with the oblate-face forward. Drag results from the present tests are compared with those for various other shapes from other sources. The drag results for the sphere and the oblate spheroid were predicted accurately over the supersonic and hypersonic speed range using impact methods.

The results indicated some conditions where the drag was affected by changes in the afterbody pressure due to a shock reflection from the tunnel wall. This effect disappeared when the Mach number was increased for a given sphere size or when the sphere size was decreased for a given Mach number. Drag measurements and Schlieren photographs are presented that show the possibility of obtaining inaccurate data when tests are made with a sphere too large for the test section size and Mach number.

Introduction

Blunt shapes are of interest for use as aerodynamic decelerators for aerobraking systems or as reentry vehicles. For such applications, the drag and stability characteristics must be determined for a wide range of operating conditions. Past studies (references 1 to 5) point out some of the problems that may be encountered in determining the aerodynamics of sphere-like shapes. These problems are generally associated with unsteady flow conditions resulting from the blunt shapes. The past studies have included both free-flight tests and tests in wind tunnels. While both of these techniques are of value, it is believed that wind-tunnel testing may provide for better control of test conditions. The intent of the present paper is to supplement the aerodynamic data base for spheres and spheroids through the presentation of some previously unpublished experimental wind-tunnel results for such shapes over a Mach number range

from 0.6 to 10.5. In addition, the supersonic drag values are compared with values calculated by impact methods.

Symbols

A	cross-sectional area at the maximum diameter
A_c	cross-sectional area of balance chamber
a.c.	aerodynamic center location
C_D	drag coefficient, drag/qA
C_{D_c}	balance chamber drag coefficient, $(p_{ts} - p_c) A_c / qA$
C_{L_α}	lift curve slope
d	diameter of sphere
M	free-stream test section Mach number
p_c	static pressure in balance chamber
p_{ts}	static pressure in test section
q	free-stream dynamic pressure
R	free-stream test section Reynolds number per foot
α	angle of attack, degrees

Models and Tests

The geometry of the test models is shown in Figure 1. The sphere models had diameters of 6, 9, and 12 inches. The 6-inch oblate spheroid was derived from the basic spherical shape but with the forward face blunted as indicated. Each model had a cutout in the rear to accommodate the housing for a strain-gage balance which, in turn, was mounted to a sting support strut. Several strain-gage balances were used in order to match the drag-beam load limit to the expected drag level of the different models. Balance-chamber pressure was measured by means of a single static-pressure orifice located in the balance chamber. The estimated accuracy of the drag coefficients is about 0.01 based on repeatability of the data.

The angle of attack was corrected for deflection of the balance and sting due to loads and for tunnel airflow angularity. The drag values were adjusted to

correspond to free-stream static pressure acting over the base cutout region. Tests of the spheres were made at zero angle of attack. Tests of the oblate spheroid were made at angles of attack from -4 to 10 degrees. Schlieren photographs were made for most of the test runs.

The tests were made in three different wind tunnels at the Langley Research Center. Descriptions of these tunnels may be found in Reference 6. Tests were made of the 6-inch sphere and oblate spheroid in the 8-Foot Transonic Pressure Tunnel for Mach numbers from 0.60 to 1.20 at Reynolds numbers of 3.0 and 5.53 million per foot. The tunnel is a single-return closed-circuit type with a 7.1-foot square test section that is capable of providing continuous Mach number variations from 0.20 to 1.30.

Tests were made of each model in the Unitary Plan Wind Tunnel at Mach numbers from 1.50 to 4.63 for a Reynolds number range from 1.0 to 6.5 million per foot. The tunnel is of the continuous-flow, asymmetric sliding-block type and there are two test sections, each 4-feet square and 7 feet long. One test section covers a Mach number range from 1.47 to 2.86 and the other, a Mach number range from 2.29 to 4.63.

Tests were made of the 6-inch sphere and oblate spheroid in the Continuous-Flow Hypersonic Tunnel in the continuous-flow mode at a Mach number of 10.5 for Reynolds numbers from 0.2 to 1.0 million per foot. The tunnel is a variable-pressure, return-flow facility with a 31-inch square test section. The test core is 14 inches square. Some limited results for a 3-inch and a 1-inch sphere at hypersonic speeds are also included.

Presentation of Results

Discussion

Transonic Results

The variations of drag with Mach number for the transonic tests are presented in Figure 2 for the sphere and the oblate spheroid for a Reynolds number of 3 million per foot. The drag results show a general increase with increasing Mach number with the oblate spheroid producing the higher values. The drag variations are somewhat irregular because of the compressibility effects on the poorly streamlined shapes. Schlieren photographs (Fig. 3) show local sonic flow near the maximum diameter of the sphere at M=0.60 which is approximately the critical Mach number for a sphere. The disturbance becomes more pronounced with increasing Mach number. A local normal shock is well established at M=0.80 and is coalesced into a supersonic shock on the model at M=0.95 The wake pattern for all of the transonic Mach numbers is divergent.

Supersonic Results

Effects of Sphere Size - The effects of sphere size at M =1.50 are presented in Figure 4 for a range of Reynolds numbers. The drag coefficients for the 9-inch sphere is substantially lower than that for the 6-inch sphere and the difference is reflected in the balance chamber drag coefficients. The reason for the difference can be seen in the Schlieren photographs (Fig. 5). The reflection of the bow shock from the test section walls is very close to the rear of the model and causes an increase in pressure at the model base that reduces the balance chamber drag coefficients. The flow field, as indicated in Figure 5, consists of the bow shock, the reflected shock from the top and bottom walls, the reflected shock with the side wall, the separated flow field and the wake boundary. The reflected shock, which can also be seen for the 6-inch sphere, is much further aft and has no effect on the model base. The pressure differences at the rear of the models produces wake patterns that are different - divergent for the 9-inch sphere and

slightly convergent for the 6-inch sphere. With the 12-inch sphere installed, it was not possible to establish M=1.50 flow in the test section.

The effects of sphere size at M=1.90 (Fig. 6) indicate good agreement in the drag coefficient values for the 6- and 9-inch models. The 12-inch model indicates substantially lower drag coefficient values at the lower Reynolds numbers and a hysteresis effect near a Reynolds number of about 3 million per foot where the drag results approach those for the two smaller models. The differences are again seen in the balance chamber drag. The arrows on the figure indicate the test sequence showing the hysteresis in the drag results. Schlieren photographs (Fig. 7) show that the reflected shock is well aft for the 6- and 9-inch models and the wake patterns are convergent for both models. For the 12-inch model, however, the reflected shock is close to the base and causes an unsteady pressure field that randomly produces a convergent wake or a divergent wake.

The effects of sphere size for a Mach number of 2.86 are shown in Figure 8. The drag coefficient results are similar for all three model sizes and the chamber drag is quite small. The Schlieren photographs (Fig. 9) indicate similar convergent wake patterns for each model and the reflected shock is not visible.

The effects of sphere size for a Mach number of 4.63 are illustrated in Figure 10. The drag coefficient values are essentially the same for all three models and the balance chamber drag was negligible. The Schlieren photographs (Fig. 11) show similar convergent wake patterns and the reflected shocks are well downstream.

It is apparent from these results that, even though supersonic flow may be established in the test section, there are cases when the reflected shock from the model may affect the pressure over the rear of the model and result in erroneous drag values. Such conditions disappear, of course, as the model size is decreased for a given Mach number or as the Mach number is increased for a given model size.

Hypersonic Results

The variation of drag coefficient with Reynolds number for the hypersonic tests (Fig. 12) show the drag level to be essentially invariant with Reynolds number above about 0.5 million per foot. At lower Reynolds number it is believed that the results are affected by tunnel blockage. This belief appears substantiated by the results shown from some unreported tests for smaller diameter spheres. A single test point for the oblate spheroid at R=0.7 million per foot indicates a slightly higher level of drag than that for the sphere.

Aerodynamics for the Oblate Spheroid

Some aerodynamic characteristics for the oblate spheroid are presented in Figure 13 for Mach numbers from 1.5 to 10.5. The drag coefficient for the oblate spheroid decreases very slightly with increasing M as does that for the sphere and the values are about 10 percent higher than for the sphere. The lift curve slope variation with M is similar to that for conventional airfoils except for being inverted. The negative lift curve slope results from the shape of the oblate spheroid. As the angle of attack is increased for this shape the curvature of the upper surface decreases while the curvature of the lower surface increases. Thus the shape behaves like an inverted airfoil. The oblate shape also produces a pitching moment as the angle of attack is varied. The variations of lift and pitching moment with angle of attack were linear for the test range from -4 to 10 degrees. By dividing the lift curve slope into the pitching moment curve slope, the aerodynamic center (a.c.) was determined and referenced to the nose of the basic sphere. The a.c. variation with M thus obtained for the oblate spheroid is rearward up to about M=5 but then begins to move forward. In order to have inherent static longitudinal stability when the lift curve slope is negative, it is necessary that the a.c. be forward of the center of gravity. It is, therefore, interesting to note that, at the higher Mach numbers, it may be possible to attain inherent positive static stability with the oblate shape.

Effects of Shape

The variation of the drag coefficients with Mach number for the sphere and the oblate spheroid are shown in Figure 14 for the transonic and supersonic tests. The results indicate drag values for the oblate spheroid that are about 10 percent higher than those for the sphere over the speed range. For comparison, the drag characteristics for various other shapes as obtained from some unpublished results from the Langley Unitary Plan Wind Tunnel at supersonic speeds for a test Reynolds number of 2.5 million per foot are also presented in Figure 14. A flat-faced cylinder and a reentry Gemini capsule show substantially higher drag than the sphere or the spheroid whereas a reentry shape and an exit Gemini capsule have considerably lower drag.

Comparisons with Other Results

Experimental - The experimental sphere drag results from the present tests are compared in Figure 15 with a summary of sphere drag test results from a variety of sources as compiled by Hoerner (Ref. 1). These data are for conditions above the critical Reynolds number. The comparison indicates close agreement and presumably could be used to establish the level of sphere drag over the range from subsonic speeds up to M=10.5.

Calculated - The calculated drag results for the sphere and the oblate spheroid at supersonic and hypersonic speeds were obtained through the use of Reference 7. Computer-generated drawings of the sphere and the spheroid are

shown in Figure 16. The comparison of experimental and calculated drag results is presented in Figure 17. The drag in the impact region (forward face) was calculated by use of the Modified Newtonian method for both the sphere and the spheroid. The drag in the shadow region (rear face) was calculated by two different methods. One was the Prandtl-Meyer expansion from free-stream method. The comparison is reasonably good - the Mach number trend being essentially exact and the calculated values being only about 5 percent higher for both the sphere and the spheroid. The second method used in the shadow region assumed that the base pressure coefficient was equal to $-1/M^2$. These results indicate almost exact agreement for the Mach number range from 1.90 to 4.63 but the calculated results at M=10.5 were the same for both methods. Skin friction values for all cases were calculated for a turbulent boundary layer by the method of Spaulding and Chi.

Concluding Remarks

It has been the purpose of this paper to assess the aerodynamics of a sphere and an oblate spheroid over a Mach number range from 0.60 to 10.5. Comparisons are made with results from various sources as well as with some calculated results. Some concluding observations are:

- The results for an oblate spheroid indicated drag values about 10 percent higher than those for a sphere.
- Results for the oblate spheroid indicated the possibility of attaining inherent positive static stability at high Mach numbers.
- The experimental drag results for the sphere were in good agreement with the results from a variety of other experimental sources.
- Calculated drag results for the sphere and the oblate spheroid indicated good agreement with the experimental values for the supersonic and hypersonic speed range.
- Erroneous drag values may be obtained if careful attention is not given to the relation between model size and the test conditions.

References

1. Hoerner, Sighard F.: Fluid-Dynamic Drag. Published by the Author, 1965.
2. Herrere, J. G.: Maximum Model-Size Determination and Effects of Sting Diameter on an Entry Shape and Sphere for Low Supersonic Mach-Number Testing. Technical Memorandum No. 33-191, Jet Propulsion Laboratory, California Institute of Technology, Pasadena, California, October 30, 1964.

3. Charters, A. C.; and Thomas, R. N.: The Aerodynamic Performance of Small Spheres from Subsonic to High Supersonic Velocities. Journal of Aeronautical Sciences, Vol. 12, No. 4, October 1945, Page 468.

4. Hodges, A. J.: The Drag Coefficient of Very High Velocity Spheres. Journal of Aeronautical Sciences, Vol. 24, No. 10, October 1957, Pages 755-758.

5. Berger, E.; Scholz, D.; and Schumm, M.: Coherent Vortex Structures in the Wake of a Sphere and a Circular Disk at Rest and Under Forced Vibrations. Journal of Fluids and Structures, Vol. 4, May 1990, Pages 231-257.

6. Schaefer, William T., Jr.: Characteristics of Major Active Wind Tunnels at the Langley Research Center. NASA TM X-1130, 1965.

7. Gentry, A. E.: Vol. I-Users Manual. Gentry, A. E.; and Smyth, D. N.: Vol. II-Program Formulation and Listings. Hypersonic Arbitrary Aerodynamic Computer Program (Mark III Version). Rep. DAC 61552, McDonnell Douglas Corp., April 1968. (Air Force Contract Nos. F33615 67 C 1008 and F33615 67 C 1602.) (Available from DTIC as AD 851811 and AD 861812.)

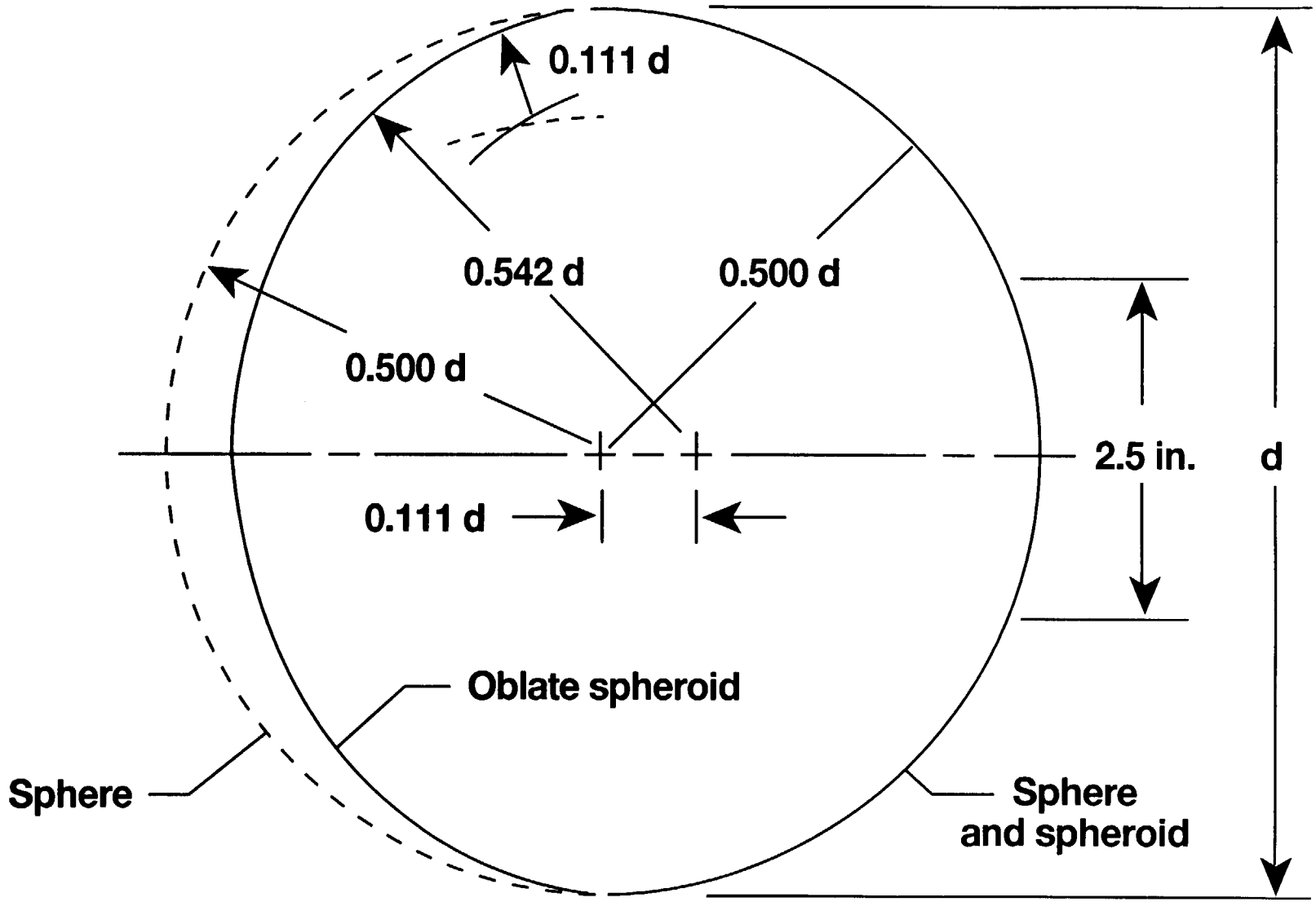

Figure 1. - Geometry of test models.

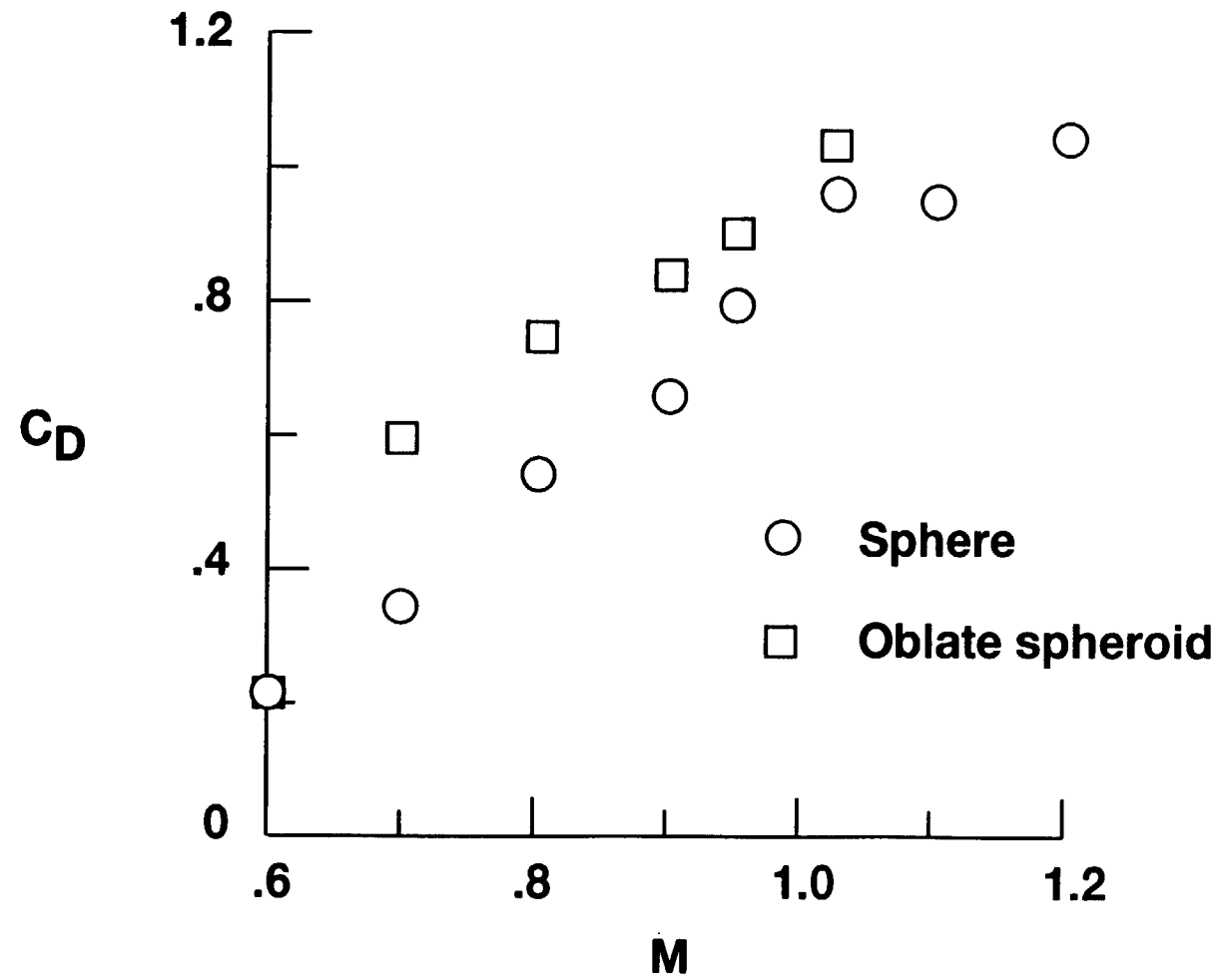

Figure 2. - Transonic drag for sphere and oblate spheroid, R=3.0 million/ft.

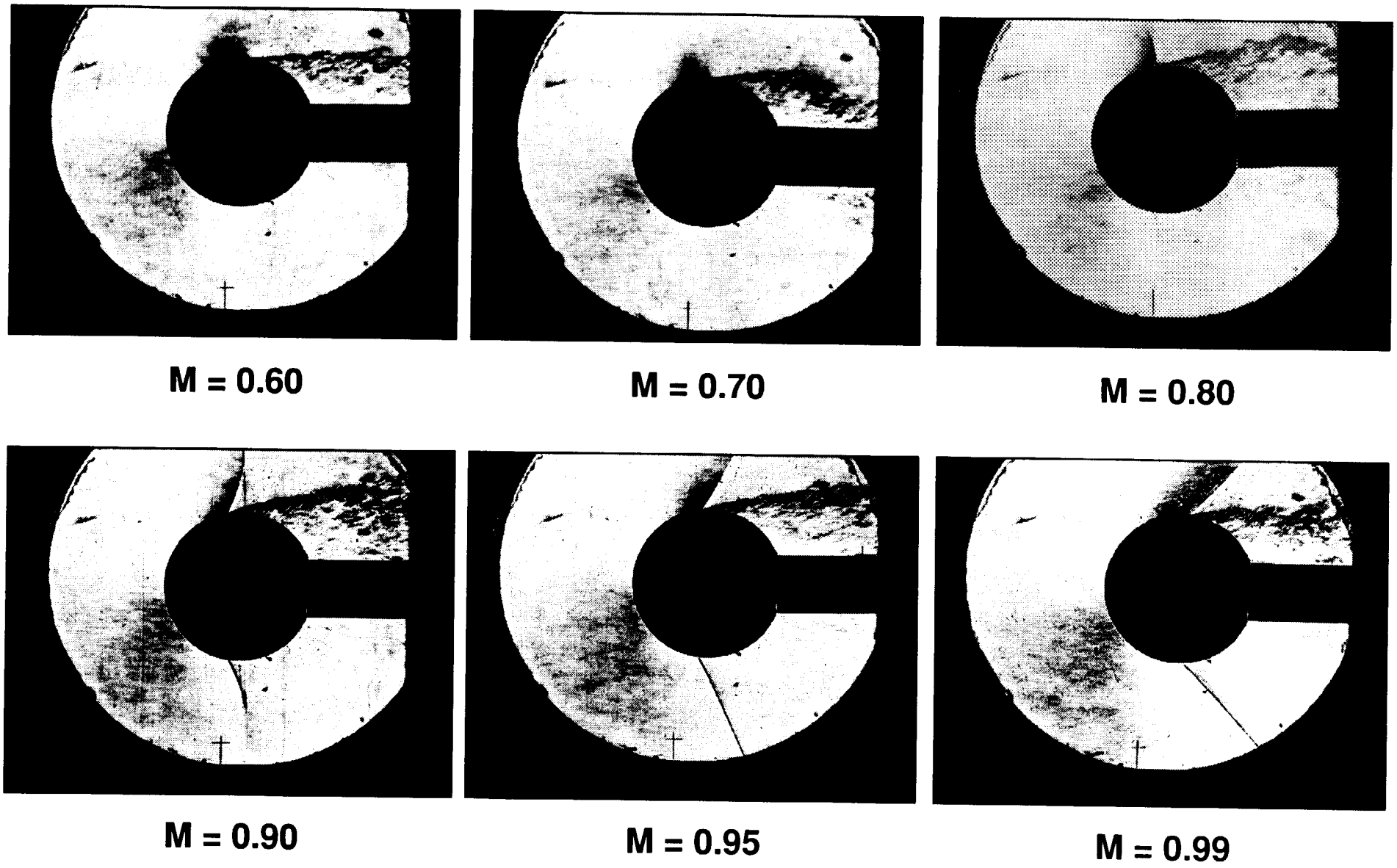

Figure 3. - Schlieren photographs for transonic speeds.

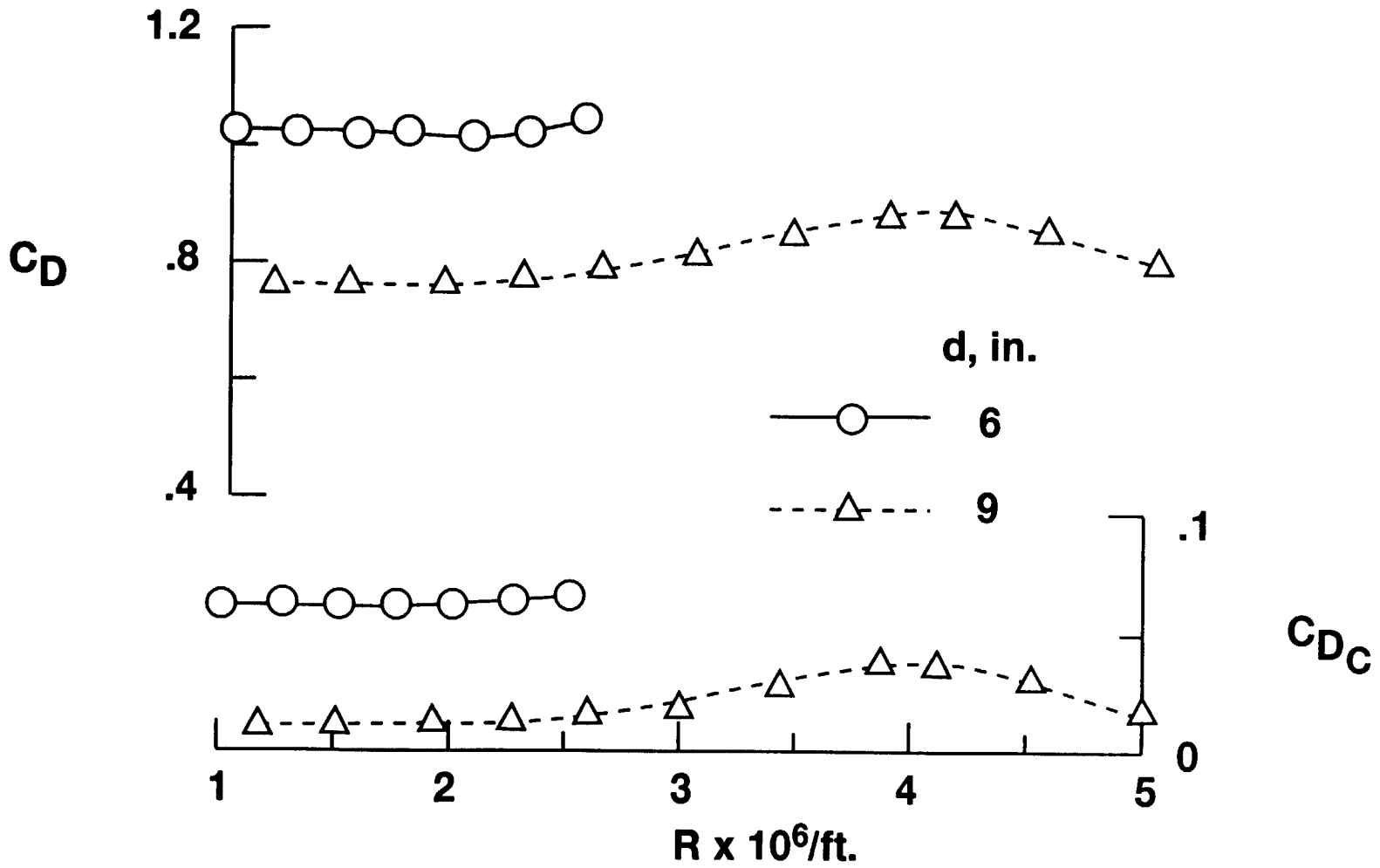

Figure 4. - Variation of sphere drag with Reynolds number, M = 1.50.

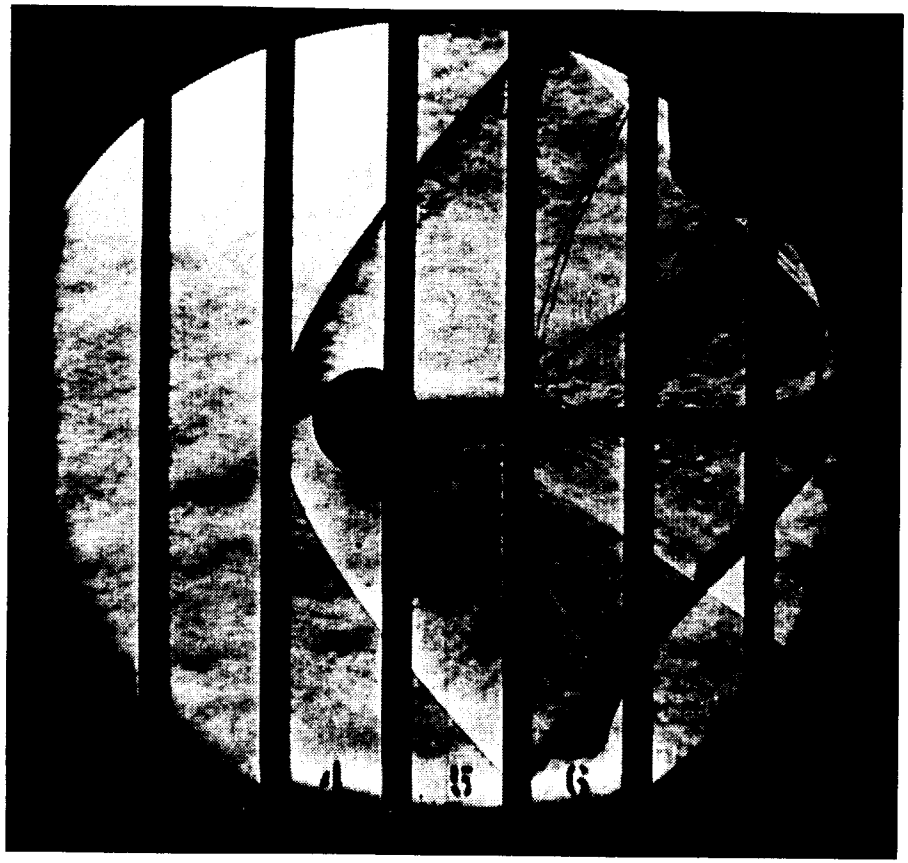

6"

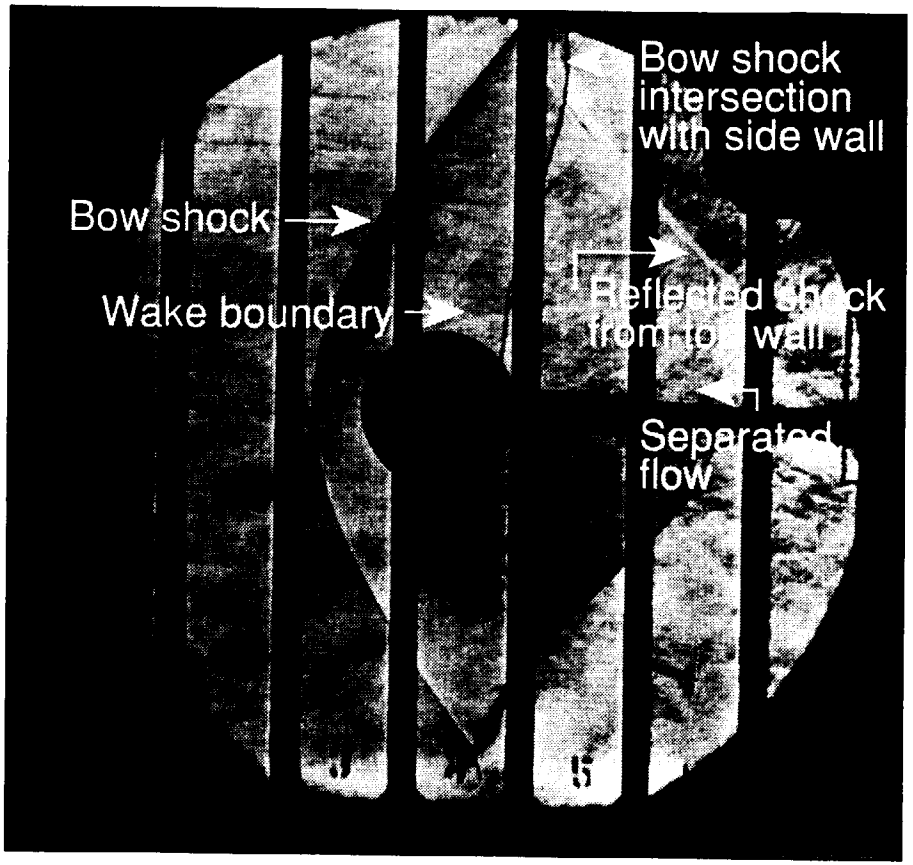

9"

Figure 5. - Schlieren photographs, M = 1.50.

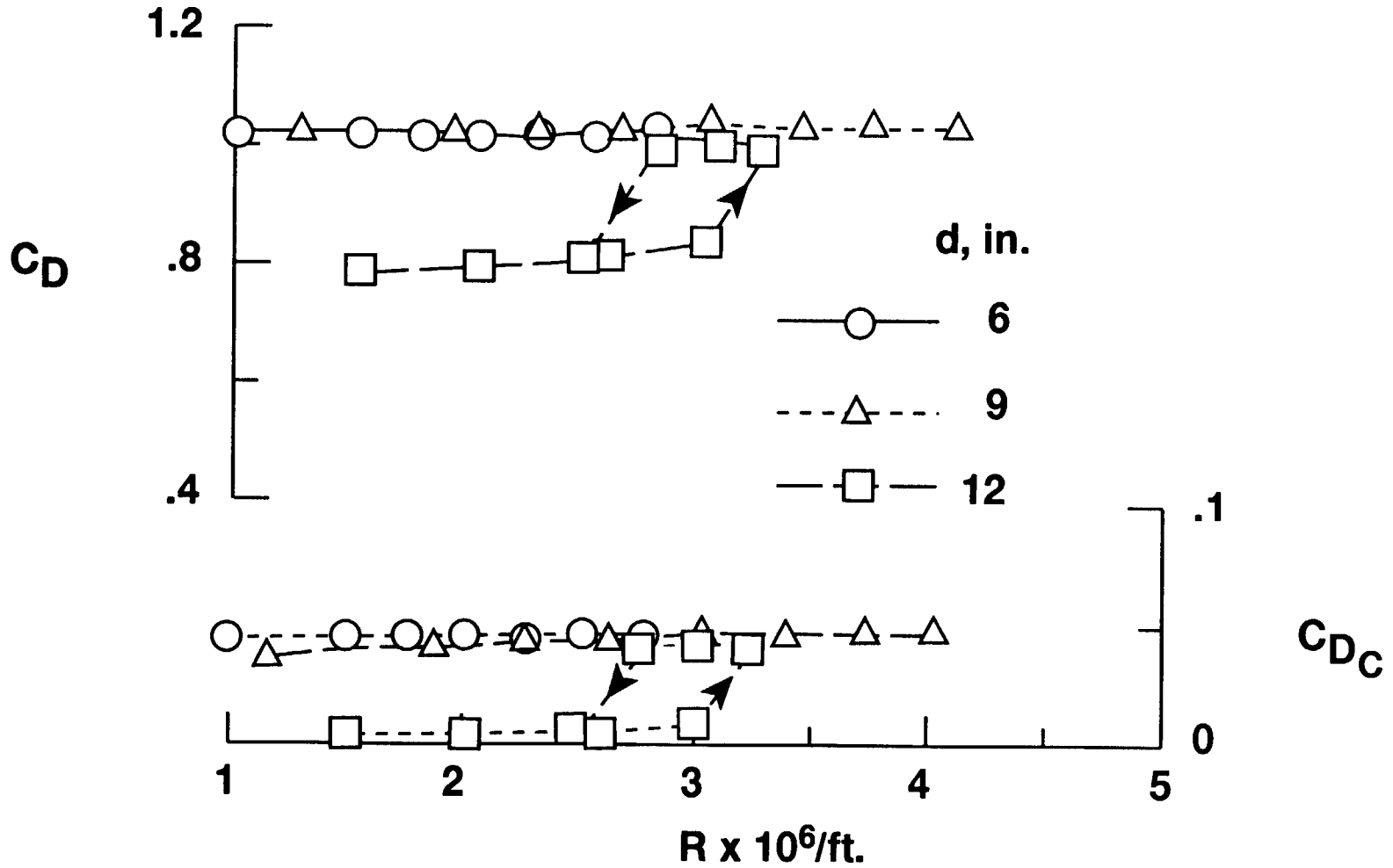

Figure 6. - Variation of sphere drag with Reynolds number, M = 1.90.

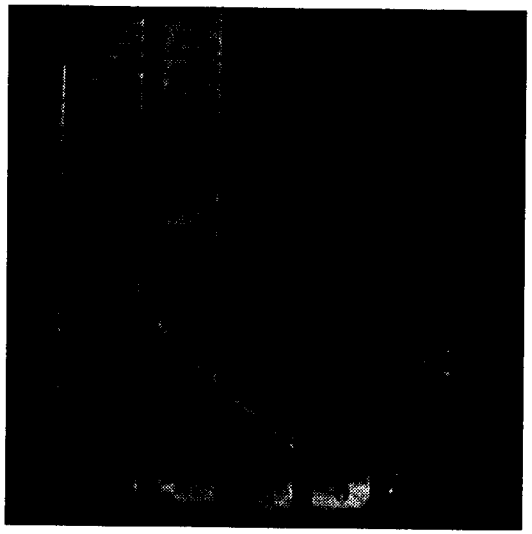

6"

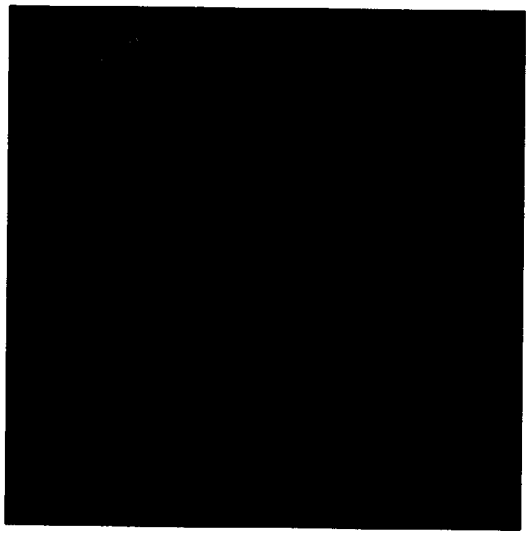

9"

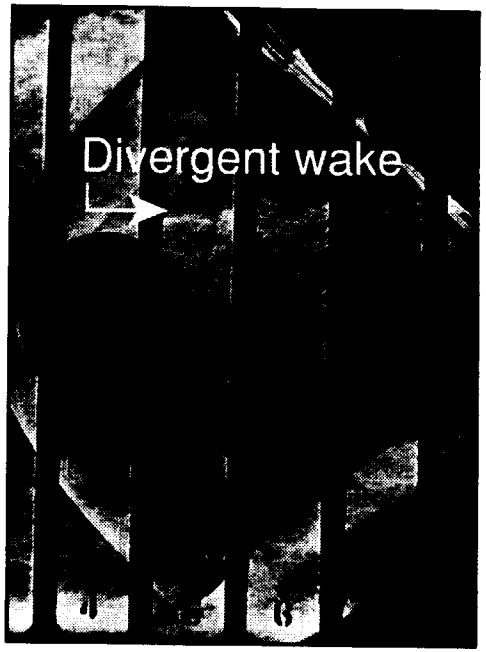

12"

12"

Figure 7. - Schlieren photographs, M = 1.90.

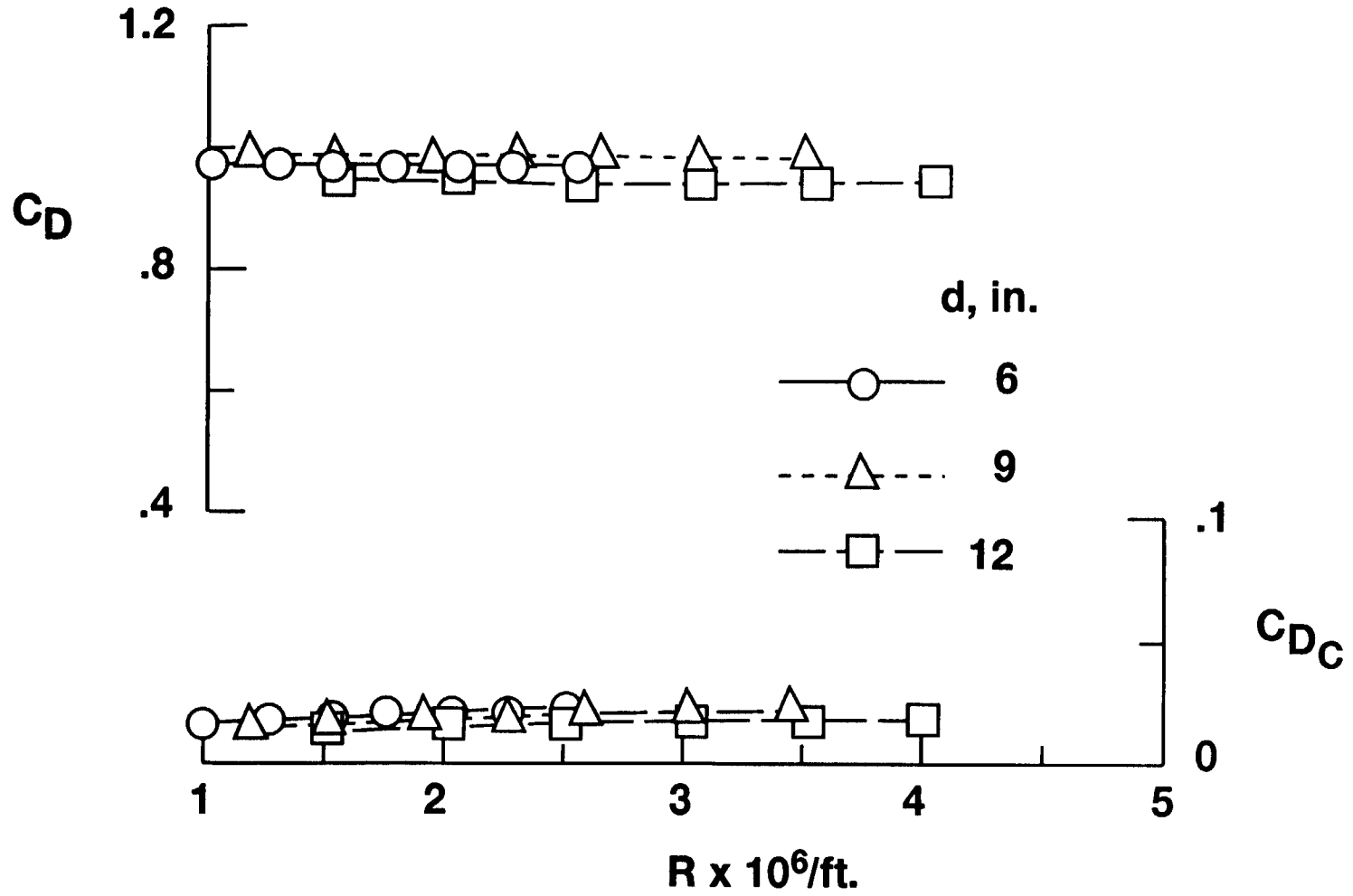

Figure 8. - Variation of sphere drag with Reynolds number, M = 2.86 .

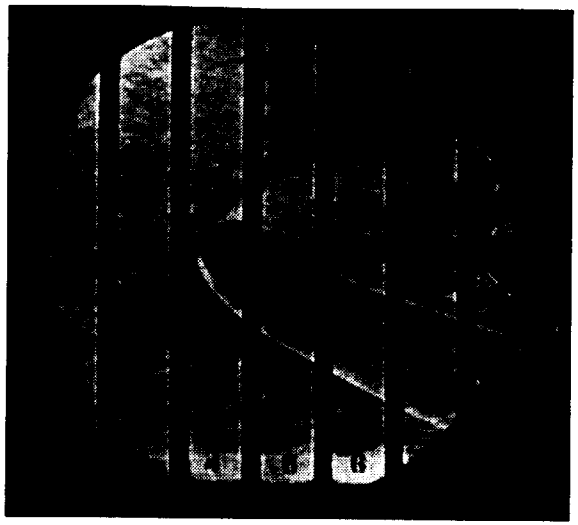

6"

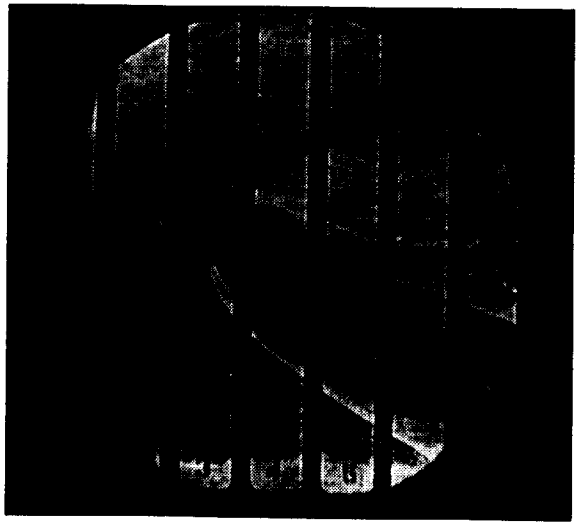

9"

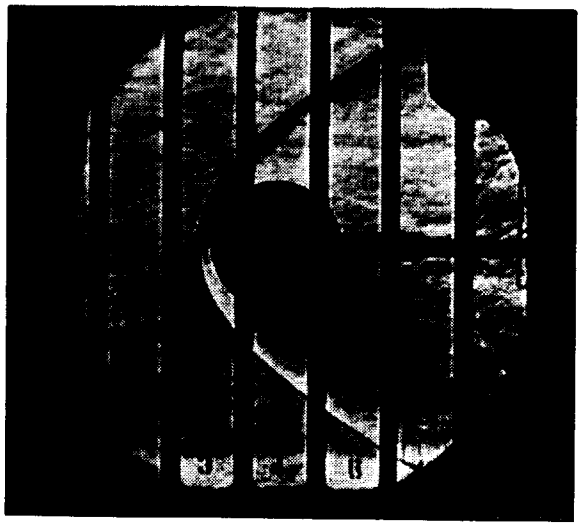

12"

Figure 9. - Schlieren photographs, M = 2.86

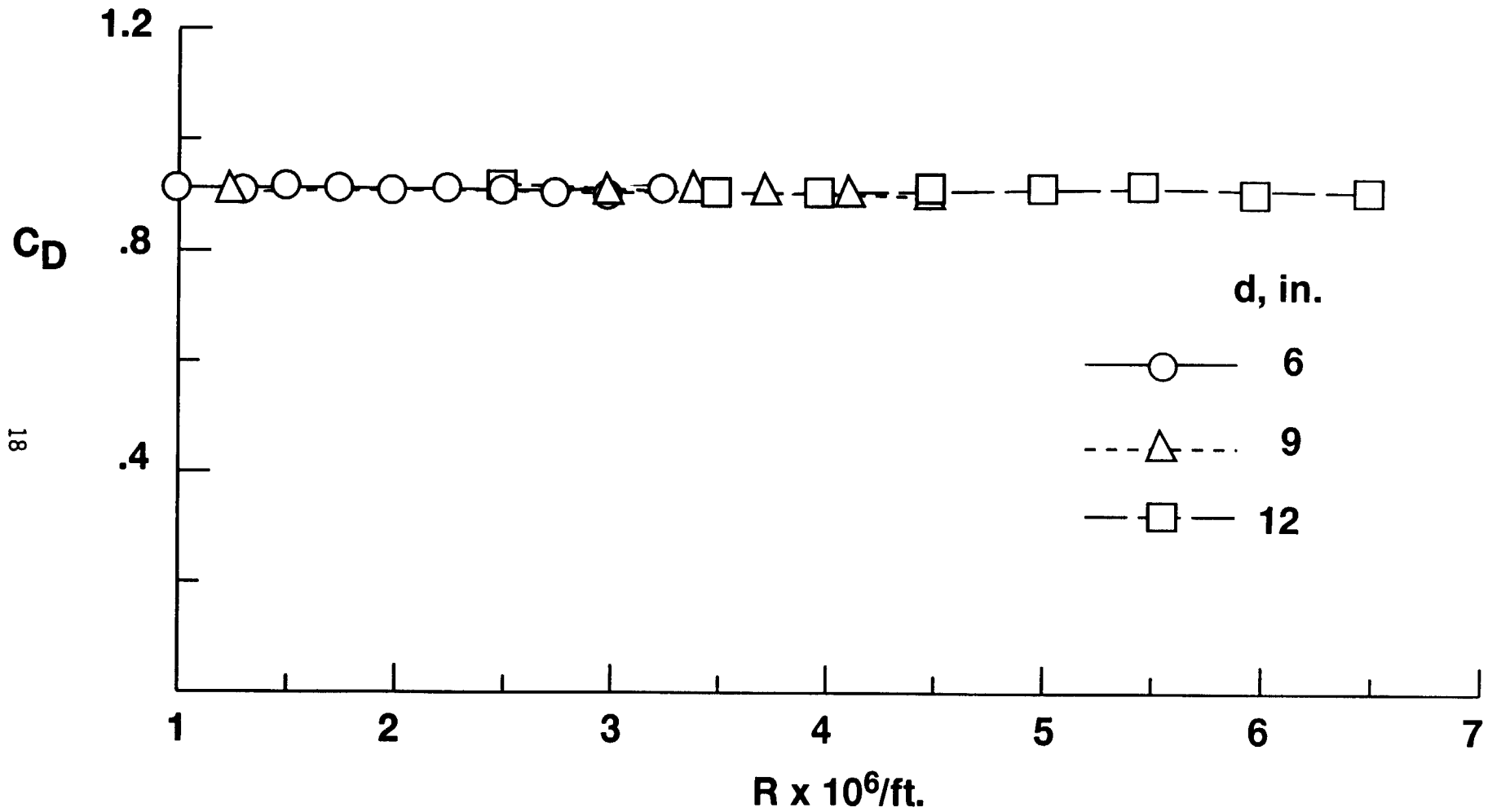

Figure 10. - Variation of sphere drag with Reynolds number, M = 4.63 .

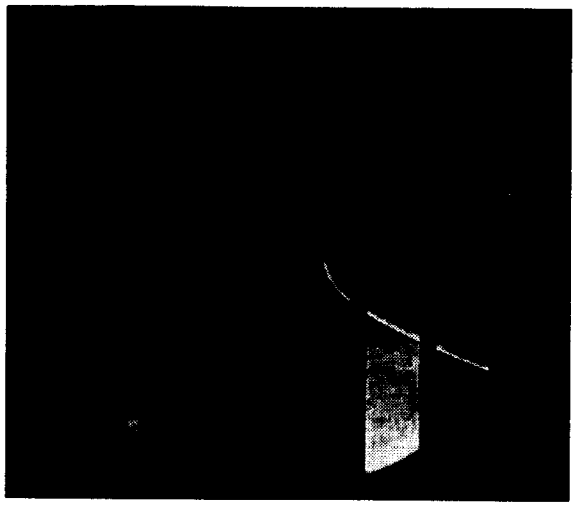

6"

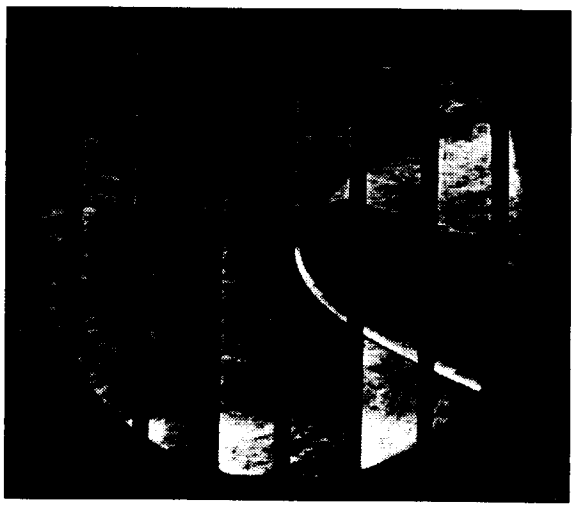

9"

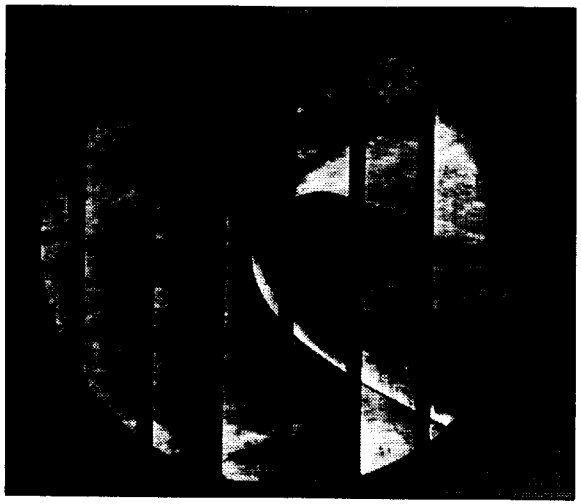

12"

Figure 11. - Schlieren photographs, M = 4.63.

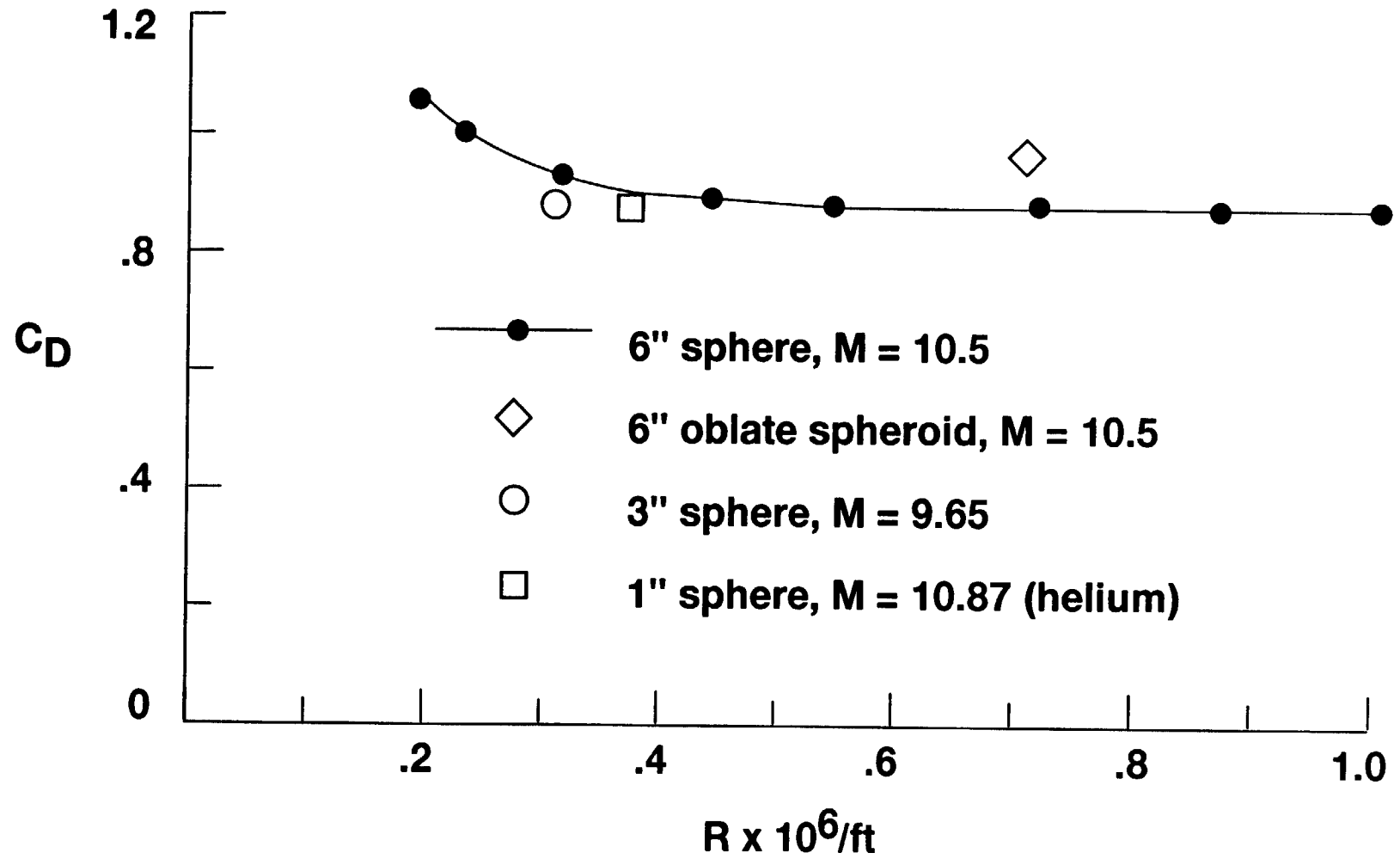

Figure 12. - Variation of hypersonic drag with Reynolds number for sphere and oblate spheroid.

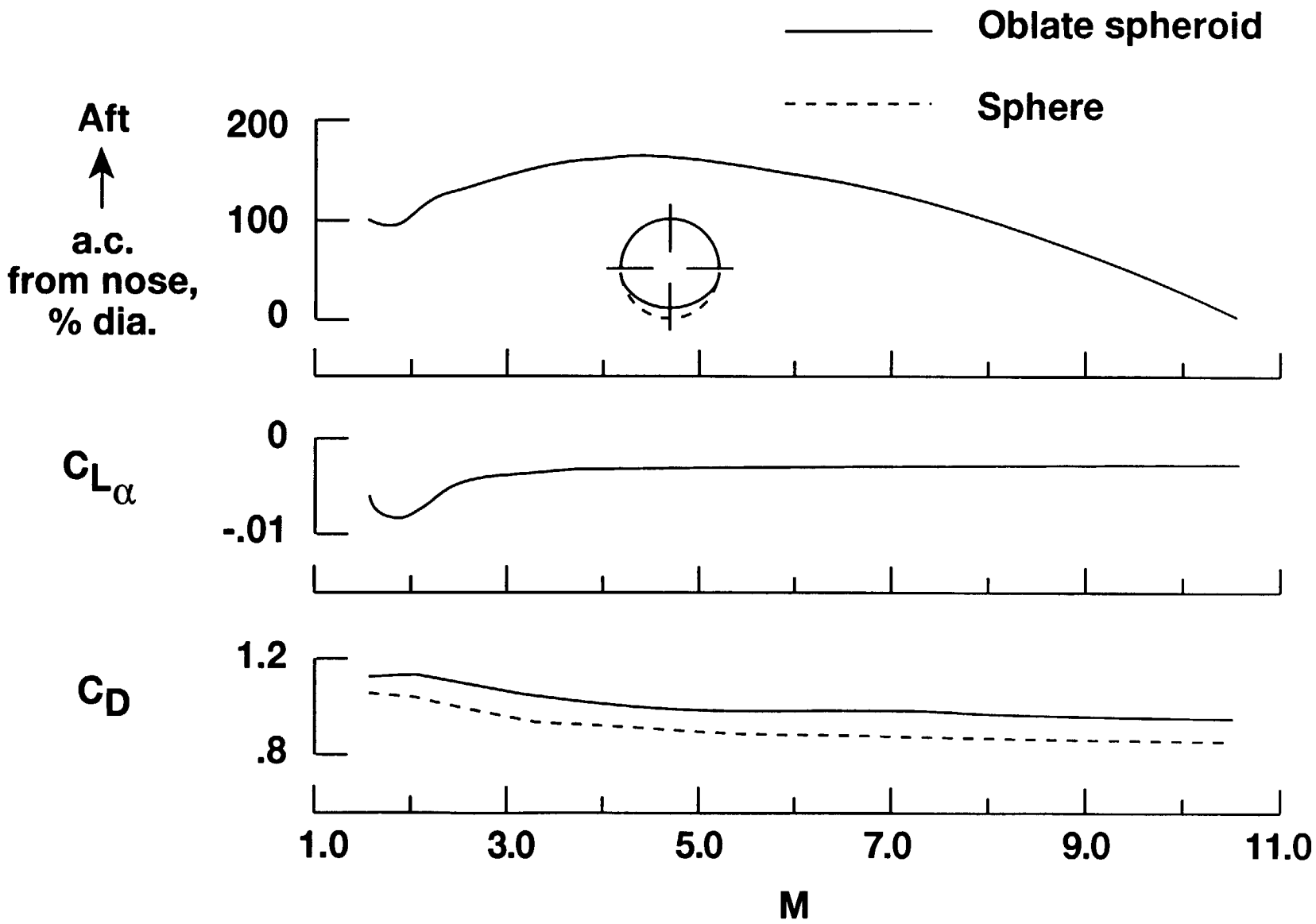

Figure 13. - Aerodynamics for the oblate spheroid.

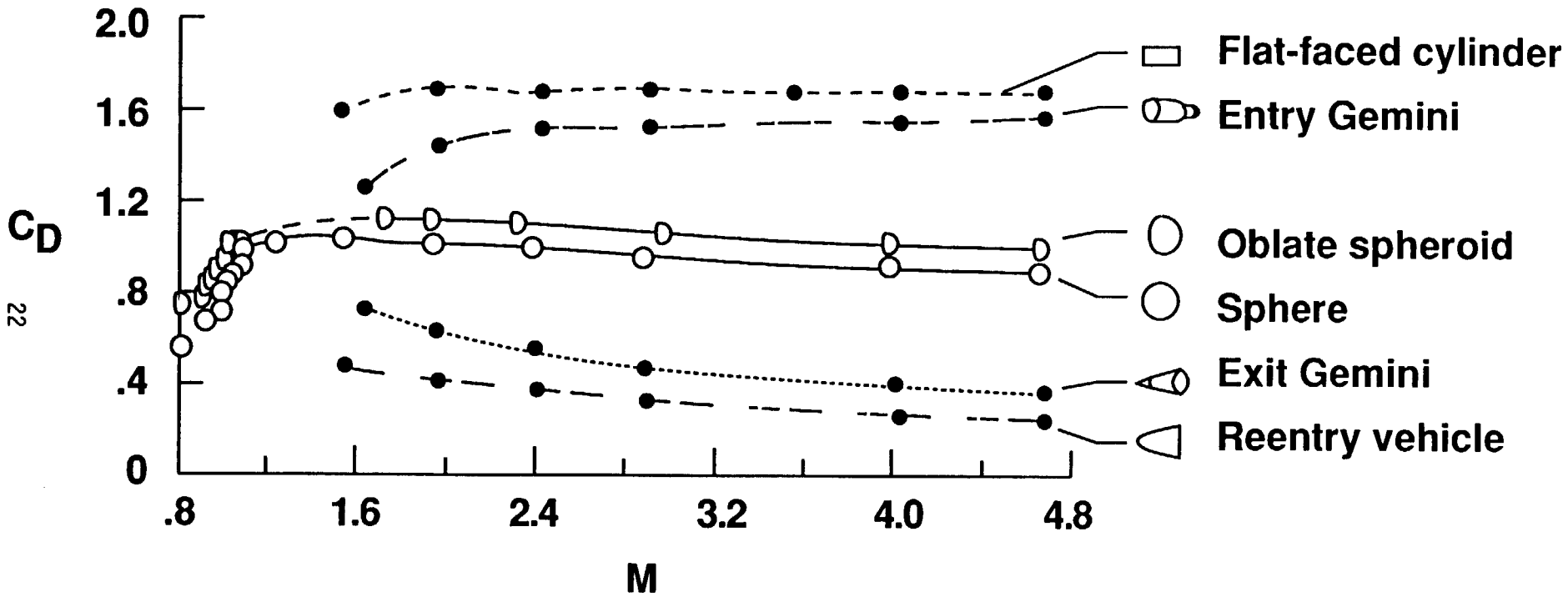

Figure 14. - Drag characteristics for various shapes.

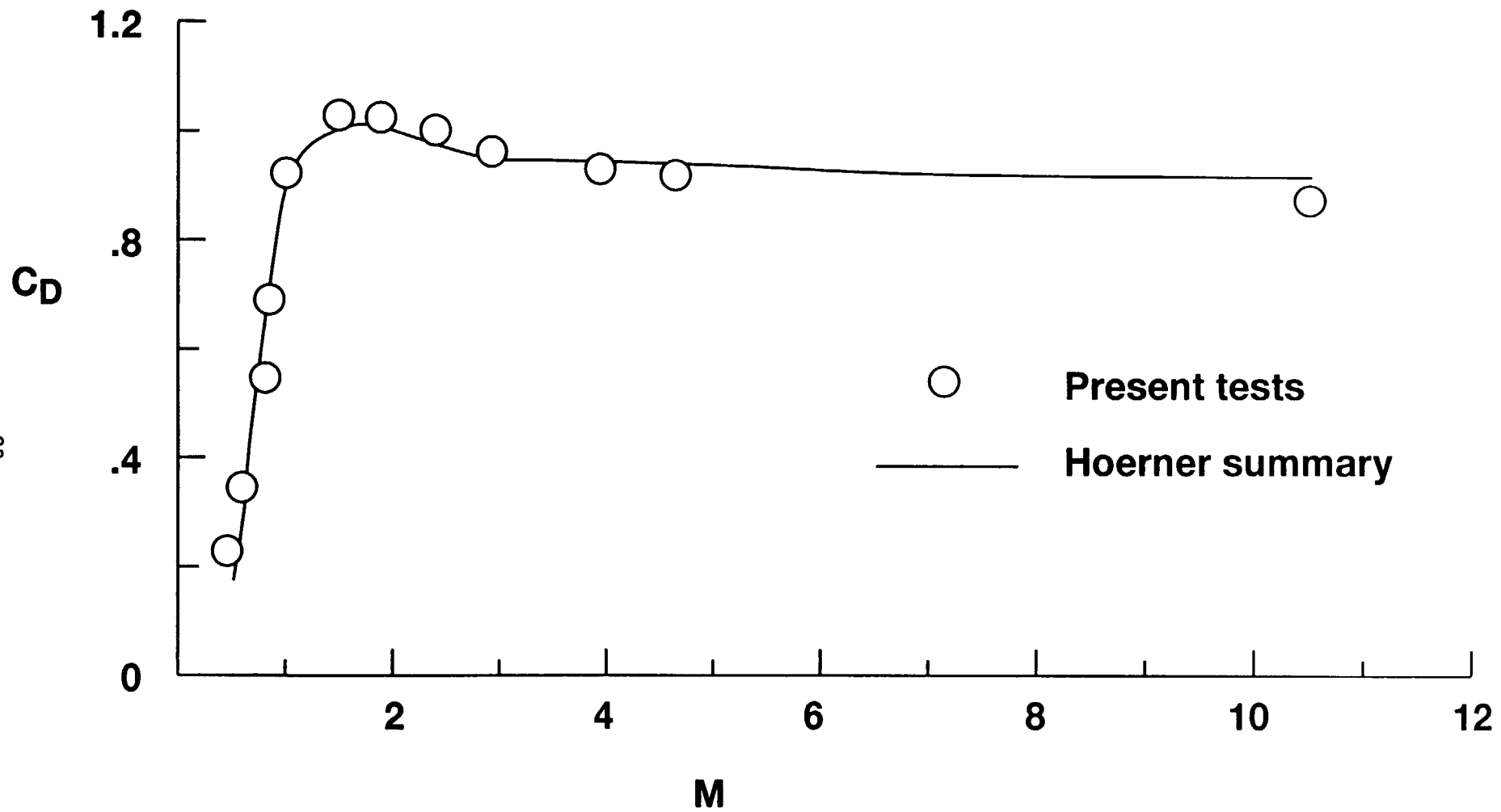

Figure 15. - Comparison with Hoerner summary.

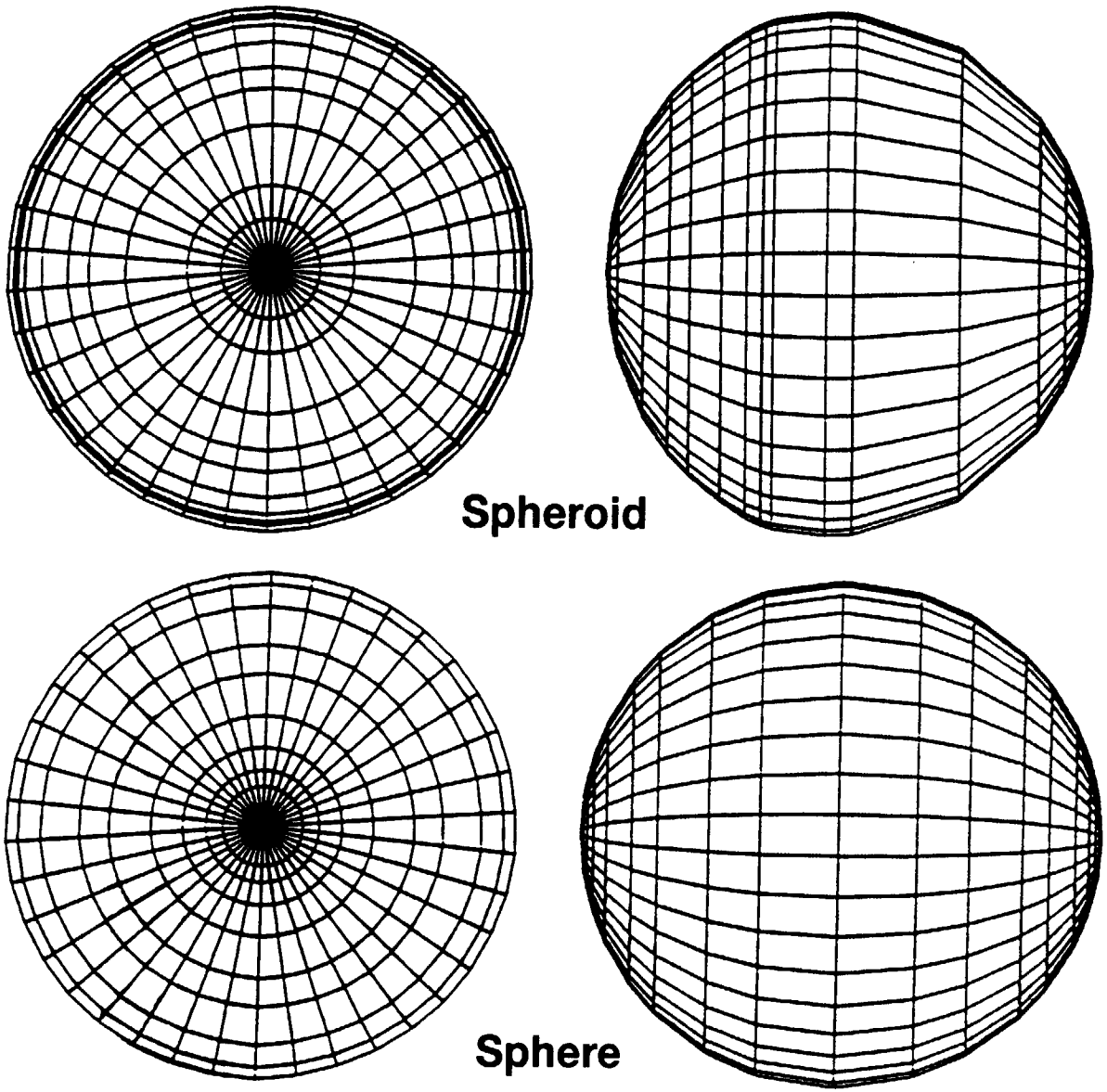

Figure 16. - Computer-generated drawings of the spheroid and sphere.

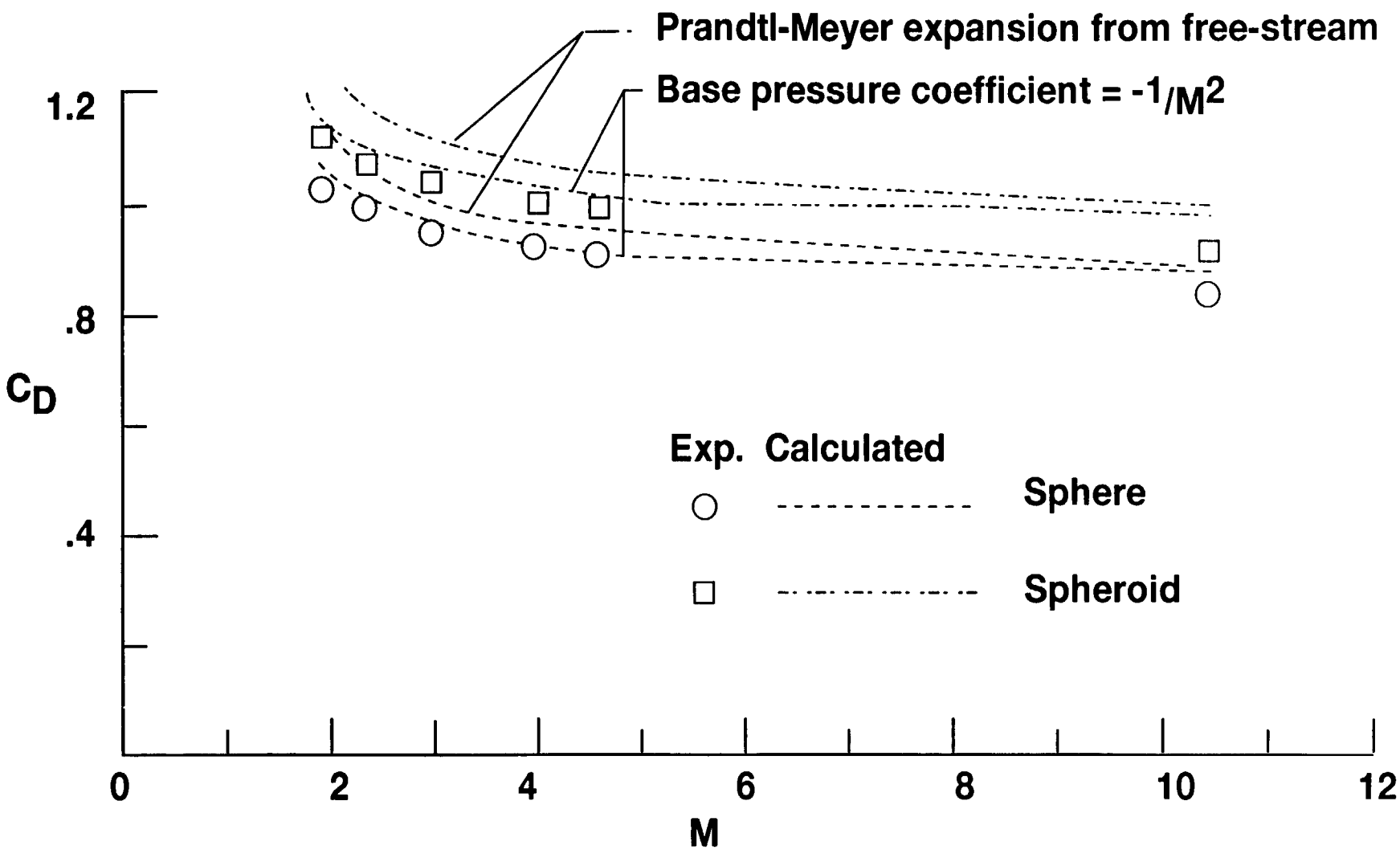

Figure 17. - Comparison with calculated results, 6" models, R=1.0 x 10^6.

REPORT DOCUMENTATION PAGE

Form Approved
OMB No. 0704-0188

1. AGENCY USE ONLY (Leave blank)	2. REPORT DATE	3. REPORT TYPE AND DATES COVERED
	August 1993	Technical Memorandum

4. TITLE AND SUBTITLE
Aerodynamics of a Sphere and an Oblate Spheroid for Mach Numbers From 0.6 to 10.5 Including Some Effects of Test Conditions

5. FUNDING NUMBERS
WU 505-69-20-01

6. AUTHOR(S)
M. Leroy Spearman and Dorothy O. Braswell

7. PERFORMING ORGANIZATION NAME(S) AND ADDRESS(ES)
NASA Langley Research Center
Hampton, VA 23681-0001

8. PERFORMING ORGANIZATION REPORT NUMBER

9. SPONSORING/MONITORING AGENCY NAME(S) AND ADDRESS(ES)
National Aeronautics and Space Administration
Washington DC 20546-0001

10. SPONSORING/MONITORING AGENCY REPORT NUMBER
NASA TM-109016

11. SUPPLEMENTARY NOTES

12a. DISTRIBUTION/AVAILABILITY STATEMENT
Unclassified - Unlimited
Subject Category 02

12b. DISTRIBUTION CODE

13. ABSTRACT *(Maximum 200 words)*

Wind-tunnel tests were made for spheres of various sizes over a range of Mach numbers and Reynolds numbers. The results indicated some conditions where the drag was affected by changes in the afterbody pressure due to a shock reflection from the tunnel wall. This effect disappeared when the Mach number was increased for a given sphere size or when the sphere size was decreased for a given Mach number. Drag measurements and Schlieren photographs are presented that show the possibility of obtaining inaccurate data when tests are made with a sphere too large for the test section size and Mach number.

Tests were also made of an oblate spheroid. The results indicated a region at high Mach numbers where inherent positive static stability might occur with the oblate-face forward. The drag results are compared with those for a sphere as well as those for various other shapes. The drag results for the oblate spheroid and the sphere are also compared with some calculated results.

14. SUBJECT TERMS
Sphere; Drag; Spheroid; Aerodynamics; Decelerators; Aerobrakes; Blunt Bodies

15. NUMBER OF PAGES
26

16. PRICE CODE
A03

17. SECURITY CLASSIFICATION OF REPORT	18. SECURITY CLASSIFICATION OF THIS PAGE	19. SECURITY CLASSIFICATION OF ABSTRACT	20. LIMITATION OF ABSTRACT
Unclassified	Unclassified	Unclassified	